Syntaxin 13 Mediates Cycling of Plasma Membrane Proteins via Tubulovesicular Recycling Endosomes

Rytis Prekeris,* Judith Klumperman,‡ Yu A. Chen,* and Richard H. Scheller*

*Howard Hughes Medical Institute, Department of Molecular and Cellular Physiology, Stanford University School of Medicine, Stanford, California 94305-5428; and ‡Medical School, University of Utrecht, Institute for Biomembranes, 3584CX Utrecht, The Netherlands

Abstract. Endocytosis-mediated recycling of plasma membrane is a critical vesicle trafficking step important in diverse biological processes. The membrane trafficking decisions and sorting events take place in a series of heterogeneous and highly dynamic organelles, the endosomes. Syntaxin 13, a recently discovered member of the syntaxin family, has been suggested to play a role in mediating endosomal trafficking. To better understand the function of syntaxin 13 we examined its intracellular distribution in nonpolarized cells. By confocal immunofluorescence and electron microscopy, syntaxin 13 is primarily found in tubular early and recycling endosomes, where it colocalizes with transferrin receptor. Additional labeling is also present in endosomal vacuoles, where it is often found in clathrin-coated membrane areas. Furthermore, anti-syntaxin 13 antibody inhibits transferrin receptor recycling in permeabilized PC12 cells. Immunoprecipitation of syntaxin 13 revealed that, in Triton X-100 extracts, syntaxin 13 is present in a complex(es) comprised of βSNAP, VAMP 2/3, and SNAP-25. This complex(es) binds exogenously added αSNAP and NSF and dissociates in the presence of ATP, but not ATPγS. These results support a role for syntaxin 13 in membrane fusion events during the recycling of plasma membrane proteins.

Key words: vesicular transport • endosomes • protein recycling • membrane trafficking • syntaxin

---

Biological membranes are used to establish functional compartments in eucaryotic organisms. The plasma membrane serves as an efficient and specific filter separating the cytoplasm from the extracellular space. As a part of mechanisms used to maintain homeostasis, cells constantly internalize plasma membrane which often includes molecules from the outside world. The best characterized mechanism of entry into the cell, endocytosis, occurs mainly through the formation of clathrin-coated vesicles (43, 44). A key event in this process is recruitment of cytosolic clathrin to the membrane, where it associates with protein complexes called adaptor proteins (12, 44). Many of the membrane receptors for extracellular ligands, such as transferrin (Tf),[1] low-density lipoprotein, and epidermal growth factor (38, 39, 59) become highly concentrated in clathrin-coated vesicles. After endocytosis, internalized proteins, lipids, and solutes are recycled back to the cell surface or routed to the degradative pathway. The membrane trafficking decisions and sorting events take place in a series of heterogeneous and highly dynamic organelles, the endosomes (38, 47). Separation of recycling proteins from proteins destined for lysosomal degradation takes place, at least in part, within early endosomes (EE), also known as sorting endosomes, located in the periphery of the cell (26, 37). The EE is a compartment comprised of two general domains, a vacuolar domain adjacent to a network of tubules and vesicles which can be dispersed throughout the cytoplasm (38). Recycling proteins enter these tubular extensions by a process which appears to involve clathrin coat-dependent budding. The vacuolar domain, on the other hand, contains proteins destined for degradation, and either directly matures into the late endosomes (LE) and lysosomes, or shuttles proteins to these organelles through endosomal carrier vesicles. From the EE, recycling molecules can be rapidly shuttled back to the plasma membrane or continue to the separate tubulovesicular compartment located in the pericentriolar region of cell, known as recycling endosomes (RE) (21) or peri-Golgi recycling compartment (27, 29). The transit through RE proceeds with slower kinetics than transport

Address correspondence to R.H. Scheller, Howard Hughes Medical Institute, Department of Molecular and Cellular Physiology, Stanford University School of Medicine, Stanford, CA 94305-5428. Tel.: (650) 723-9075. Fax: (650) 725-4436. E-mail: scheller@cmgm.stanford.edu

1. *Abbreviations used in this paper:* BFA, brefeldin A; EE, early endosomes; LE, late endosomes; NEM, *N*-ethylmaleimide; NRK, normal rat kidney; NSF, *N*-ethylmaleimide–sensitive factor; PNS, postnuclear supernatant; RE, recycling endosomes; SLO, streptolysin-O, SNAP, soluble NSF attachment protein; SNAP-25, synaptosomal-associated protein of 25 kD; SNARE, soluble NSF attachment protein receptor; t-SNARE, target SNARE; Tf, transferrin; TfR, transferrin receptor; VAMP, vesicle-associated membrane protein.

through EE (14, 49) and depends on an intact microtubular network (20, 27, 29, 67). The definition of the boundaries between the highly dynamic EE and RE remains controversial, and at least in some cell types all endosomes have been proposed to form a continuous tubulovesicular network (28). Indeed, the RE retain the highly tubular nature observed in parts of the EE. Thus, it remains to be determined whether EE and RE comprise truly distinct organelles. On the other hand, the existence of proteins which are restricted to specific classes of endosomes argues in favor of the existence of a biochemically and functionally distinct set of compartments. For instance, the small GTPase rab4 (14) and rab5 (11) are associated only with the EE, whereas rab11 (60) is thought to be specific for the RE. Moreover, although the EE contain proteins destined for recycling as well as degradation, the RE contain proteins largely destined for transport back to the cell surface (67).

Understanding the intricate and dynamic organization of endosomal compartments is dependent on our ability to establish relationships between the morphological descriptions and biochemical definitions of the different trafficking steps through the endocytic pathway. In recent years a set of proteins has emerged whose role is to mediate and regulate intracellular membrane fusion events. Vesicle-associated membrane proteins (VAMPs) and syntaxins, also known as soluble *N*-ethylmaleimide–sensitive factor (NSF) attachment protein (SNAP) receptors or SNAREs, have been suggested to be important in determining the specificity of vesicle transport and to mediate membrane fusion (6, 54, 55). Soluble NSF attachment protein receptor (SNARE) proteins were initially divided into two functional classes, target (t)-SNAREs of the syntaxin family and vesicle (v)-SNAREs of the VAMP family, based on their putative role as vesicular or target membrane proteins, respectively. The membrane fusion event, at least in nerve terminals, has been proposed to be mediated by formation of a very stable core complex, comprised of VAMP2, syntaxin 1, and synaptosomal-associated protein of 25 kD (SNAP-25), which brings the membranes together in direct opposition (22, 33). It is believed that the same principle applies to nonneuronal cells, where syntaxin 1 and VAMP2 can be substituted with the other members of the SNARE family. NSF and α/βSNAP proteins then function as chaperones to dissociate the complex after fusion or before SNARE complex formation. A key feature of the SNARE hypothesis is that v-SNARE interacts with an appropriate t-SNARE to form organelle specific docking and fusion complexes, and that the specificity of these interactions ensures that transport vesicles fuse only with an appropriate acceptor membranes (55). However, the specificity of SNARE pairing has not been investigated sufficiently to confirm or disprove this hypothesis. Recent studies of yeast and mammalian SNAREs suggest that the pairing may not be of the high specificity originally envisioned. For instance, the mammalian Golgi t-SNARE syntaxin 5 forms a mutually exclusive complex with Gos28 or rbet1/sec22b and membrin (24). Likewise, the yeast vacuolar t-SNARE Vam3p, which interacts with Nyv1p in homotypical vacuolar fusion (40) is also needed for the docking and fusion of several other transport vesicles, namely autophagosomes, intermediates from the pre-vacuolar compartment, and vesicles delivering alkaline phosphatase to the vacuoles (15). In addition, the yeast v-SNARE Vti1p interacts with several t-SNAREs, including Pep12p (Golgi to endosomes), Sed5p (ER to Golgi), and Tgi1p/Tgi2p (*trans*-Golgi). These data suggest that individual SNAREs operate in multiple trafficking steps and in multiple complexes with other proteins. Thus, an understanding of the proteins that regulate vesicular trafficking relies not only on the identification of t- and v-SNARES, but also on the characterization of the combinatorial interactions between them.

Despite the progress in our understanding of ER to Golgi vesicular trafficking and exocytosis, very little is known about molecular events involved in regulating the docking and fusion in the endocytic pathway of mammalian cells. Only one SNARE, VAMP3, has been shown to have an endosomal localization (34). However, it remains to be determined which endosomal syntaxins interact with VAMP3. So far three putative endosomal t-SNAREs have been characterized: syntaxin 7 (63, 66), syntaxin 12 (57), and syntaxin 13 (1). Syntaxin 12 and syntaxin 13 share 98% homology and are likely to be orthologues. All three syntaxins were cloned using sequences obtained from a human expressed sequence tag database and are suggested to play a role in endosomal trafficking based on their homology to Pep12p, the yeast t-SNARE involved in Golgi to endosome trafficking (5). However, only syntaxin 7 has been linked to the endocytic pathway, through its localization on EE (66). Moreover, the other regulatory proteins which interact with syntaxins 7 and 13 remain to be determined.

Here we characterize the subcellular distribution and function of syntaxin 13, a putative endosomal SNARE. By immunofluorescence and electron microscopy we localized syntaxin 13 to tubular extensions of early endosomes, as well as recycling endosomes. Moreover, using a Tf recycling assay in permeabilized PC12 cells, we demonstrate that syntaxin 13 is directly involved in the recycling of plasma membrane proteins. Finally, using immunoprecipitation and microsequencing techniques, we identify putative syntaxin 13–interacting proteins.

Materials and Methods

Materials and Antibodies

Cell culture reagents were obtained from Life Technologies (Gaithersburg, MD) unless otherwise specified. Human Tf-biotin was obtained from Sigma Chemical Co. (St. Louis, MO). Dextran-biotin, Texas red-labeled Tf, and FITC-labeled dextran were purchased from Molecular Probes (Eugene, OR). Enhanced chemiluminescence reagents were obtained from Amersham Corp. (Buckinghamshire, UK). ImmunoPure ABC biotin detection kit was purchased from Pierce Chemical Co. (Rockford, IL). Human diferric [^{125}I]Tf was obtained from DuPont NEN (Wilmington, DE). Miscellaneous chemicals were obtained from Sigma Chemical Co. and Fisher Biochemicals (Santa Clara, CA).

Anti-syntaxin 13 antibodies were prepared by immunizations with bacterially expressed full-length cytoplasmic domain of syntaxin 13. Polyclonal antibodies were then affinity purified from rabbit antisera as described previously (9). Monoclonal antibodies were obtained from the corresponding hybridoma cell lines generated by fusion of NS-1 mouse myeloma cells with spleens cells from immunized BALB/c mouse as described previously (9). Anti-syntaxin 6 monoclonal, anti-syntaxin 1A monoclonal, and anti-syntaxin 5 polyclonal were described previously (9, 25, 30). Mouse anti-Tf receptor antibodies were purchased from Zymed Lab-

oratories Inc. (South San Francisco, CA). Mouse monoclonal anticlathrin antibody was obtained from Transduction Laboratories (Lexington, KY). Texas red-labeled anti–rabbit IgG and FITC-labeled anti–mice IgG antibodies were obtained from Jackson ImmunoResearch Laboratories (West Grove, PA).

Anti-syntaxin 13 polyclonal antibody Fab fragments were generated using papain cross-linked to 6% beaded agarose (Pierce Chemical Co.) as described in manufacturer's instructions. The efficiency of the digestion was confirmed by SDS-PAGE separation followed by Coomassie staining.

Cell Culture and Internalization Assays

CHO, NRK, NIH3T3, and AtT-20 cells were grown in DME media supplemented with 10% FCS, 100 U/ml penicillin, and 100 μg/ml streptomycin in humidified incubators with 5% CO_2 at 37°C. PC12 cells were grown in DME media supplemented with 5% FCS, 10% horse serum, 100 U/ml penicillin, and 100 μg/ml streptomycin in humidified incubators with 10% CO_2 at 37°C. Primary hippocampal CA3/CA1 embryonic cultures were obtained and maintained as described previously (3). Before each internalization experiment cells were incubated for 1 h in internalization media, consisting from DME with 50 mM Hepes, pH 7.4, and 3% BSA. Labeled Tf or dextran was then added at a concentration of 60 μg/ml or 1 mg/ml respectively, and incubated as described in Results. Cells were then chilled on ice, washed extensively with ice-cold PBS, and processed either for immunofluorescence analysis or centrifugation on velocity gradients. For pulse–chase experiments, after a PBS wash cells were overlaid with internalization media containing unlabeled Tf or dextran and incubated at 37°C as described in Results. Cells were then washed again with ice-cold PBS and processed for immunofluorescence or velocity centrifugation.

Glycerol Velocity Gradients

Rat brains or spleens were homogenized in 20 mM Hepes, pH 7.4, containing 120 mM KCl, 2 mM EDTA, 2 mM EGTA, 1 mM DTT, 0.1 mM PMSF, 2 μg/ml leupeptin, 4 μg/ml aprotinin, and 0.8 μg/ml pepstatin, using a glass-teflon homogenizer. Postnuclear supernatant (PNS) was obtained by centrifuging the homogenate at 2,000 *g* for 10 min twice. PNS was then extracted with 1% Triton X-100 and insoluble material sedimented at 100,000 *g* for 1 h. Glycerol gradients were prepared as described previously (24). Samples were either control membrane extracts (see above), or extracts preincubated for 30 min with 250 μg/ml each of histidine-tagged NSF and histidine-tagged αSNAP (55), and either 500 μM ATPγS or 500 μM ATP with 8 mM magnesium chloride.

Immunoprecipitation Experiments and Protein Sequencing

For immunoprecipitations from rat brain, PNS Triton X-100 extract was prepared as described above and then preabsorbed for 2 h at 4°C with protein A–Sepharose beads. Immunoprecipitations were carried overnight at 4°C in the presence of affinity-purified anti-syntaxin 13 rabbit polyclonal antibody coupled to protein A–Sepharose (24). As a control, protein A–Sepharose coated with IgG was used. After the binding step the beads were washed four times with homogenization buffer containing 1% Triton X-100 (first three washes) or 0.2% Triton X-100 (final wash). Washed beads were then resuspended in SDS sample buffer and eluted proteins separated on SDS-PAGE.

The proteins shown in Fig. 9 were sequenced as described previously (9, 24). In brief, proteins immunoprecipitated from 200 ml of rat brain Triton X-100 extract were pooled, separated on SDS-PAGE, and then Coomassie stained. Protein bands were cut out, trypsin digested, and then eluted. HPLC purification of peptides and Edman microsequencing were carried out by D. Winan at the Stanford University PAN Facility.

In Vitro Recycling of Tf in Permeabilized PC12 Cells

To measure Tf recycling, PC12 cells were starved for 1 h in DME media containing 1% BSA and 50 mM Hepes, pH 7.4, before adding 4 μg/ml (4:1 ratio between unlabeled and [I^{125}]labeled) human diferric Tf. Cells were incubated at 37°C for 30 min and chilled immediately on ice. Cells were then washed several times with ice-cold 25 mM Hepes, pH 7.4, containing 70 mM sucrose, 120 mM NaCl, 4.8 mM KCl, 1.3 mM $CaCl_2$, and 1.2 mM $MgSO_4$, and removed from the plate by resuspending in KGlu/BSA buffer (20 mM K acetate, 105 mM K glutamate, 50 mM Hepes, pH 7.4, 2 mM EGTA, and 0.1% BSA). PC12 cells were permeabilized using streptolysin-O (SLO) (Murex Diagnostics, Dartford, UK). In brief, 40 U of reduced lyophilized SLO was resuspended in 25 ml of ice-cold H_2O and then concentrated to 4 U/ml using Stirred Cell concentrator (Amicon, Beverly, MA). Cells were incubated with 1 U/ml SLO on ice for 10 min and then washed extensively and incubated at 37°C for 7.5 min followed by 1 h of incubation on ice. Cells were then washed four times with ice-cold KGlu/BSA buffer. Alternatively where indicated, resuspended PC12 cells were permeabilized by cracking and cytosol washed out as described previously (23). PC12 "ghosts" were then resuspended in KGlu/BSA buffer to achieve concentration 2.5×10^7 cells/ml. Where indicated, 3 mg/ml cytosol was added. In all cases KGlu/BSA buffer was supplemented with 0.5 mM ATP and an ATP regeneration system (80 mM creatine phosphate, 9 U/ml creatine kinase). Tf recycling was induced by incubating samples at 37°C for specified amounts of time. Where indicated, PC12 "ghosts" were preincubated for 1 h on ice with anti-syntaxin 1A, anti-syntaxin 5, and anti-syntaxin 13 antibodies. Where indicated, Fab fragments of anti-syntaxin 13 antibodies were used. After incubation at 37°C PC12 cells were sedimented by microcentrifuging at 5,000 *g* for 5 min. Obtained supernatant represents the released Tf. Where PC12 cells were permeabilized by "cracking," supernatant was precleared by centrifuging at 100,000 *g* for 1 h to sediment endosomes which leaked from the permeabilized cells. Leaked endosomes constituted ~12% of total internalized Tf. To determine plasma membrane-bound Tf, cells were extracted with PBS containing 0.2 M glycine, pH 2.5, for 30 min. Nonextractable Tf represents internalized Tf. The amounts of [^{125}I]Tf were determined by scintillation counting and expressed either as percentage of total Tf (the sum of released, membrane-associated, and internalized Tf for each sample) or as percentage of the control (total Tf release in the presence of cytosol).

In vitro [^{3}H]noradrenaline release assay was done as described previously (4, 23). Where indicated, anti-syntaxin 1 or anti-syntaxin 13 antibody were preincubated for 1 h at 4°C with PC12 cell "ghosts" before adding cytosol and Ca^{2+}.

To prepare cytosol for Tf recycling and noradrenaline release assays, fresh rat brains were homogenized in 25 mM Hepes, pH 7.4, containing 115 mM potassium acetate, 2.5 mM Mg-acetate, 0.1 mM EGTA, 2 mM DTT, 2 μg/ml leupeptin, 4 μg/ml aprotinin, and 0.8 μg/ml pepstatin. This homogenate was then subjected to centrifuging at 10,000 *g* for 20 min, followed by centrifuging at 100,000 *g* for 45 min. Cytosol was then flash-frozen in liquid nitrogen and stored at −80°C. The protein concentration was determined by the Bradford assay according to manufacturer's instructions (Bio-Rad, Hercules, CA). Where indicated, cytosol was pretreated with 2 mM *N*-ethylmaleimide (NEM) for 30 min on ice.

Immunofluorescence Microscopy

Low-density NIH3T3, CHO, NRK, AtT-20, and PC12 cells were fixed with 4% paraformaldehyde for 25 min. Cells were then permeabilized in 4% saponin and nonspecific sites blocked with PBS containing 0.2% BSA, 4% saponin, and 1% goat serum. Antisera were used at the following dilutions: anti-syntaxin 13 polyclonal antibody at 1 μg/ml; anti-Tf receptor monoclonal antibody at 1 μg/ml; anti-syntaxin 6 monoclonal antibody at 2 μg/ml; FITC-labeled anti–mouse IgG and Texas red-labeled anti–rabbit IgG were used at 7.5 μg/ml. After washes, samples were mounted in VectaShield (Vector Laboratories, Burlingame, CA). Immunofluorescence localization was performed on NRK, CHO, AtT-20, NIH3T3, and PC12 cells using Molecular Dynamics laser confocal imaging system (Beckman Center Imaging Facility, Stanford University).

Immunogold Labeling of Ultrathin Cryosections

CHO cells were prepared for ultrathin cryosections and immunogold labeling as described previously (53). In short, cells were fixed in 2% paraformaldehyde/0.2% glutaraldehyde in 0.1 M phosphate buffer for 2 h at room temperature and then post fixed overnight at 4°C in 2% paraformaldehyde. Then cells were washed with 0.02 M glycine in PBS, scraped off the dish, and pelleted in 10% gelatin in PBS, which was solidified on ice and cut into small blocks. After overnight infiltration with 2.3 M sucrose at 4°C for cryoprotection, blocks were mounted on aluminium pins and frozen in liquid nitrogen. Ultrathin cryosections were picked up in a mixture of sucrose and methyl cellulose. The rabbit polyclonal antibody against syntaxin 13 was directly visualized by binding to receptor A–gold, whereas the mouse derived anti-Tf receptor and clathrin antibodies were visualized in a two-step procedure using rabbit anti–mouse IgG antibody (Dako, Copenhagen, Denmark) to provide binding sites for protein A–gold.

To establish the distribution pattern of syntaxin 13, areas of the grids were selected that contained cells exhibiting a good ultrastructure. At a magnification of 25,000, these areas were scanned along a fixed track and all gold particles within a distance of 30 nm from a membrane were counted as positive and assigned to the compartment over which they were located. Three independent quantitations were performed and 508 gold particles were counted in total. The distribution of gold particles was expressed as percentage of total gold particles found over a specific compartment. To establish the degree of colocalization of syntaxin 13 and TfR, sections were double-immunogold labeled for TfR (10-nm gold) and syntaxin 13 (15-nm gold). Then a total of 255 syntaxin 13-positive organelles were selected and scored positive or negative for TfR. Brief quantitation in sections in which a reversed labeling procedure was followed, showed a similar degree of colocalization (data not shown).

Results

Syntaxin 13 Tissue Expression Patterns

Previously reported Northern blot analysis demonstrated that syntaxin 13 is expressed in all tissues with a relatively higher expression in brain, lung, spleen, and pancreas (1). To study the protein distribution we generated rabbit polyclonal and a mouse monoclonal (15G2) antibodies using the cytoplasmic portion of recombinant syntaxin 13 as antigen. Both antibodies recognized a single major 38-kD band in rat brain PNS (Fig. 1 *A*), which was not recognized by preimmune sera (data not shown). In some cases, a less prominent additional band of 27 kD could also be detected (Fig. 1, *A* and *B*). This band most likely represents a degradation product of full-length syntaxin 13 since it usually is not detectable in tissues that are rapidly processed for electrophoresis and becomes more prominent in samples that are slowly prepared. Both antibodies were used to analyze the distribution of syntaxin 13 protein in multiple tissues (Fig. 1 *B*). Syntaxin 13 was found to be expressed in all tissues, with relatively higher protein levels in brain, lung, spleen, thymus, and testes. This broad tissue distribution suggests that syntaxin 13 mediates a fundamental membrane trafficking event common to all cell types. Despite the abundant expression of syntaxin 13 in some tissues, others express relatively low levels of the protein. Perhaps functionally redundant isoforms substitute for syntaxin 13 in some cells. Alternatively, it is possible that some tissues including brain, spleen, lung, and pancreas have a prominent trafficking step mediated by syntaxin 13.

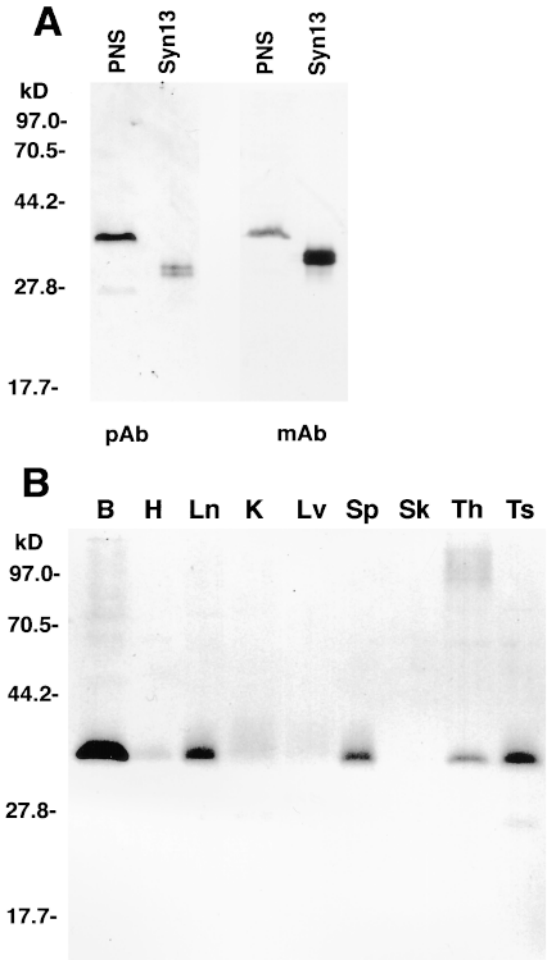

Figure 1. Syntaxin 13 is a broadly and differentially expressed SNARE protein. (*A*) Rabbit polyclonal (*pAb*) and mouse monoclonal 15G2 (*mAb*) antibodies recognize a major 38-kD band in rat brain PNS. The recombinant full-length cytoplasmic domain of syntaxin 13 (*Syn13*) was used as a positive control. (*B*) PNSs from brain (*B*), heart (*H*), lung (*Ln*), kidney (*K*), liver (*Lv*), spleen (*Sp*), skeletal muscle (*Sk*), thymus (*Th*), and testis (*Ts*) were analyzed by Western blot using mouse monoclonal 15G2 antibody. A single major band is detected at 38 kD, with the highest expression levels in brain, spleen, lung, thymus, and testis.

Syntaxin 13 Subcellular Distribution

Defining the localization of vesicle trafficking proteins is a critical step in understanding the specific function of the molecule. We previously reported that full-length, amino terminally *c-myc* epitope-tagged syntaxin 13, when transiently expressed in normal rat kidney (NRK) cells, was predominantly targeted to the post-Golgi compartment (1). To determine the localization of endogenous syntaxin 13, we stained CHO, AtT20, PC12, NRK, NIH3T3 cells, and hippocampal neurons with the affinity-purified polyclonal antibodies. Western blot analysis demonstrated that all cells used for immunofluorescence microscopy expresses syntaxin 13 (data not shown). In all nonpolarized cells syntaxin 13 was detected in small puncta throughout the cell, but primarily located in juctanuclear area (Fig. 2, *A–E*). Interestingly, in hippocampal neurons syntaxin 13 immunoreactive organelles were scattered throughout dendritic and axonal processes (Fig. 2 *F*), as identified by costaining with anti-MAP2 (dendritic marker) and anti-SV2a (axonal marker) antibodies (data not shown).

To begin a more detailed understanding of the distribution of syntaxin 13, we compared its immunostaining with that of well-characterized markers of lysosomal, endosomal, and TGN compartments. The pattern of syntaxin 13 staining almost completely overlapped with TfR known to be enriched in RE (Fig. 3, *A–C*). In contrast, lgp120, a marker for late endosomes and lysosomes, showed little colocalization with syntaxin 13 (Fig. 3, *D–F*). In most cell types, RE are located in the peri-Golgi region, juxtaposed to the Golgi stacks. Unfortunately, light microscopy does not have the resolution necessary to differentiate Golgi,

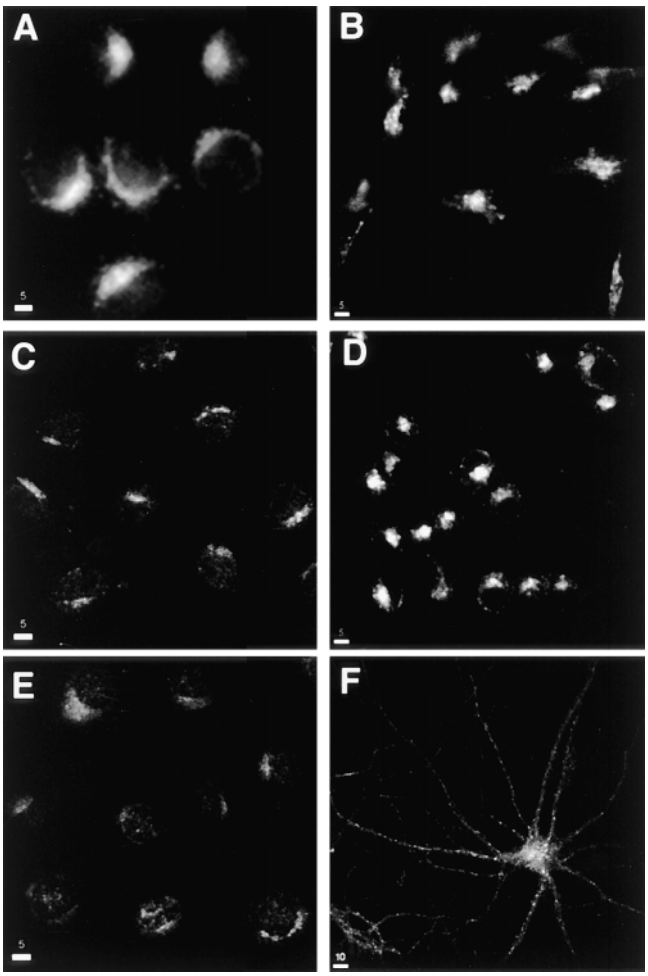

Figure 2. Syntaxin 13 localization in different cell lines. Cells were fixed with 4% paraformaldehyde, permeabilized with saponin, and stained using affinity-purified rabbit anti-syntaxin 13 antibody and followed by incubation with FITC-labeled anti–mouse IgG antibodies before processing for confocal microscopy. (*A*) CHO; (*B*) AtT-20; (*C*) NRK; (*D*) PC12; (*E*) NIH3T3; (*F*) 15 d in vitro hippocamapal neurons. Bars: (*A–E*) 5 μm; (*F*) 10 μm.

TGN, and RE compartments. Indeed, at this level of resolution, syntaxin 13 showed a significant overlap with syntaxin 6, a protein that is mainly located in the TGN (10) (Fig. 2, *G–I*), as well as Golgi protein mannosidase II (data not shown).

The dynamics of membrane proteins in the presence of brefeldin A (BFA) and nocodazole can reveal features of their native localization and life cycle. BFA causes a block in ER to Golgi trafficking resulting in the redistribution of Golgi proteins back to the ER (46). At the same time in some cells it collapses the TGN and endosomes onto the microtubule-organizing center (35, 45). Indeed, treatment of NRK cells with 5 μg/ml BFA resulted in the redistribution of syntaxin 13 staining into a compact spot in the center of the cell, where it remained colocalized with the TfR (Fig. 4, compare *A* and *B* with *C* and *D*). This result shows that syntaxin 13 is not associated with Golgi but might instead reside in the TGN and/or endosomal compartments. To further investigate this issue, we treated NRK cells with the microtubule-depolymerizing agent nocodazole. The integrity of the endosomal compartment is dependent on an intact microtubule network (67) and depolymerization of microtubules causes its disintegration into multiple vesicular structures, scattered throughout the cytoplasm of the cell. Treatment of NRK cells with nocodazole converted the syntaxin 13–positive perinuclear compartment into multiple vesicular structures (Fig. 4 *E*), characteristic of nocodazole-induced changes of endosomal markers. Indeed, most of these vesicular structures also contain the TfR (Fig. 4 *F*). Thus, the above results strongly suggest that syntaxin 13 is localized to endosomes.

Syntaxin 13 Colocalizes with Ligand-based Recycling but Not Degradative Pathways

In an effort to determine the functional localization of syntaxin 13, we followed the internalization and cycling of Texas red-labeled Tf (Tf-TxR) and fluorescein-labeled dextran (Dex-FITC) in CHO cells. Loading the cells with Tf-TxR at 37°C for 30 min resulted in a perinuclear staining pattern which is similar to that of Tf receptor and colocalizes extensively with syntaxin 13 (Fig. 5, *A–C*). When cells were incubated with Tf-TxR in the presence of 100-fold excess of unlabeled Tf, no staining was observed (data not shown) indicating the specificity of Tf-TxR uptake. Previous studies have shown that at temperatures between 15° and 22°C endocytosis does take place, but recycling is slowed, resulting in accumulation of plasma membrane proteins such as facilitative glucose transporter (GLUT4) and Tf receptor in large vesicular structures that are broadly distributed throughout the cell (50, 64). Indeed, the internalization of Tf-TxR at 15°C for 2.5 h resulted in accumulation of Tf-TxR in cytoplasmic vesicular structures (Fig. 5 *E*). Once again, these Tf-TxR–positive structures also immunostained with syntaxin 13 antibodies, confirming our previous results that Tf receptor and syntaxin 13 colocalizes to the same organelles (Fig. 5, *D–F*). Furthermore, when the 15°C block was removed by chasing the cells at 37°C for 15 min, Tf-TxR/syntaxin 13–positive structures redistributed and became indistinguishable from the previously discussed perinuclear staining pattern (Fig. 5, *G–I*).

In contrast to Tf, dextrans, metabolically inert hydrophilic polysaccharides, enter the cell mainly through fluid-phase endocytosis (16). Their biologically uncommon α-1,6-polyglucose linkages are resistant to cleavage by most endogenous glycosidases making them ideal long-term tracers for labeling late endosomes. Syntaxin 13 showed very little, if any, colocalization with Dex-FITC labeled late endosomes/lysosomes (data not shown), suggesting that the protein resides specifically in the recycling, but not degradative pathway. To confirm the immunocytochemical localization studies, we fractionated organelles purified either from dextran-biotin or Tf-biotin–labeled CHO cells. When separated on 0.2–1.5 M sucrose continuous velocity gradients, syntaxin 13 showed little cofractionation with dextran-biotin. However, all fractions containing Tf-biotin also contained syntaxin 13 consistent with our fluorescence microscopy data that syntaxin 13 is localized to the endosomes involved in protein recycling (data not shown).

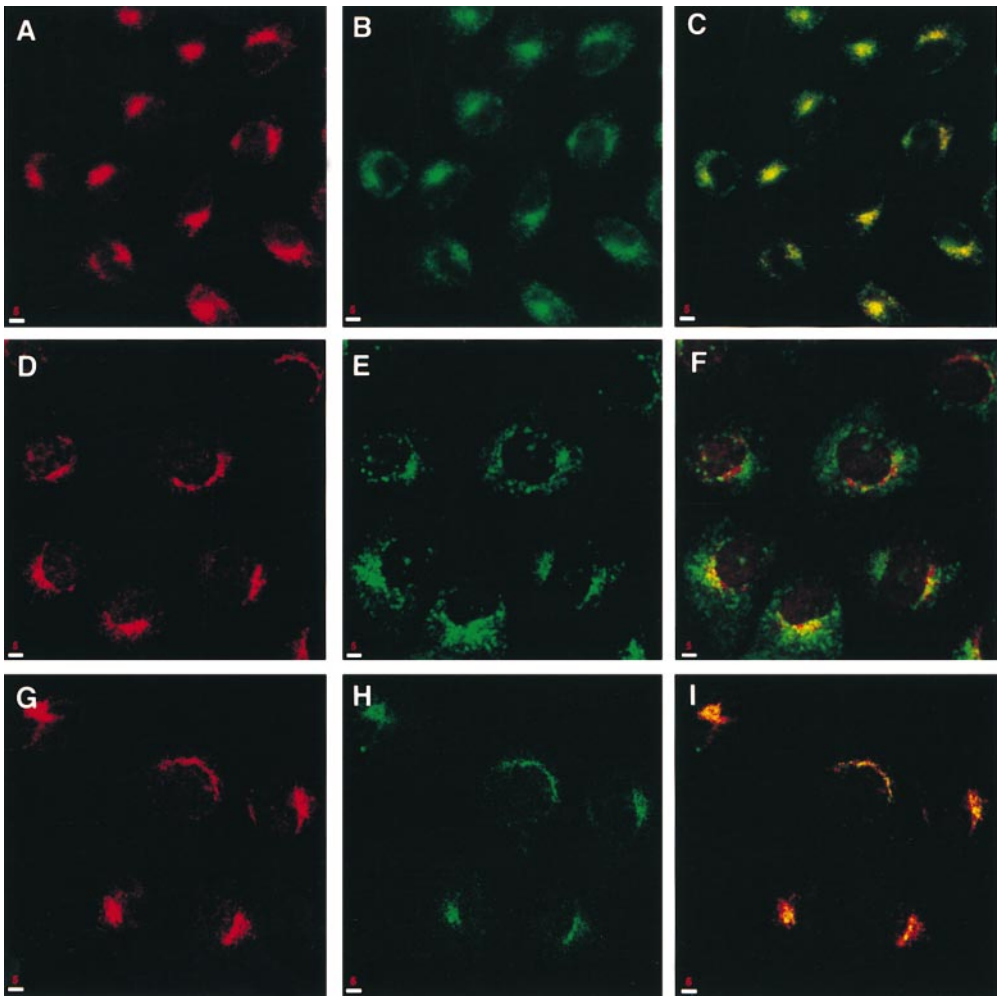

Figure 3. Syntaxin 13 colocalizes with TfR. NRK cells were fixed with 4% paraformaldehyde, permeabilized with saponin, and costained using affinity-purified rabbit anti-syntaxin 13 antibody (*A*, *D*, and *G*) and mouse monoclonal antibodies against TfR (*B*), lgp120 (*E*), and syntaxin 6 (*H*). This was followed by incubation with Texas red-labeled anti–rabbit IgG and FITC-labeled anti-mouse IgG antibodies before processing for confocal microscopy. *Yellow*, areas of overlap in merged images (*C*, *F*, and *I*). Bars, 5 μm.

Syntaxin 13 Is Localized to the Tubular Extensions of Early and Recycling Endosomes

To assess the distribution of syntaxin 13 at the subcellular level, ultrathin cryosections were prepared from CHO cells and immunogold labeled with affinity-purified polyclonal anti-syntaxin 13 antibody. Syntaxin 13 was localized to an extensive, branched network of tubules and associated buds and vesicles through the cell (Fig. 6 *A*). A small portion of these membranes was surrounded by a dense cytoplasmic coating, characteristic for the presence of clathrin. Syntaxin 13–positive membranes were found near the Golgi stack (Fig. 6 *A*) and adjacent to vacuolar endosomes. Occasionally continuities between an endosomal vacuole and syntaxin 13–positive tubules were observed (Fig. 6 *B*). Quantification of the labeling pattern revealed that the vast majority (77 ± 9%) of syntaxin 13 was found on these tubules and vesicles. Additional labeling was also found at the limiting membrane of the endosomal vacuoles (13 ± 6%), of which about one-third occurred in the areas of the membrane that were coated with clathrin (Fig. 6, *A* and *C*). Label over other compartments (ER, Golgi, and plasma membrane) was around background level.

Double-immunogold labeling of syntaxin 13 and TfR revealed a high degree of colocalization in the tubulovesicular membrane profiles, both near endosomal vacuoles and Golgi complexes (Fig. 7). Of all individual vesicles and larger tubules that were positive for syntaxin 13, ~50% were labeled for TfR as well. Finally, this double labeling revealed that syntaxin 13 was mainly present on the tubulovesicular network of EE and RE that harbored TfR as well.

Syntaxin 13 Mediates the Recycling of Plasma Membrane Proteins

The immunolocalization and subcellular fractionation data suggest that syntaxin 13 may play a role in mediating recycling of plasma membrane proteins, including TfR. To analyze Tf cycling at the molecular level, we reconstituted this process in SLO-permeabilized PC12 cells. Using this system we hoped to better understand the mechanisms of plasma membrane protein recycling and to determine the role of syntaxin 13 in this process.

To label the cells [^{125}I]Tf was internalized for 30 min at 37°C. These loading conditions label early as well as recycling endosomes (Fig. 5). In PC12 cells loaded under similar conditions with Tf-TxR, immunofluorescence microscopy demonstrated that, as in CHO and NRK cells, Tf localized to peripheral and perinuclear structures resem-

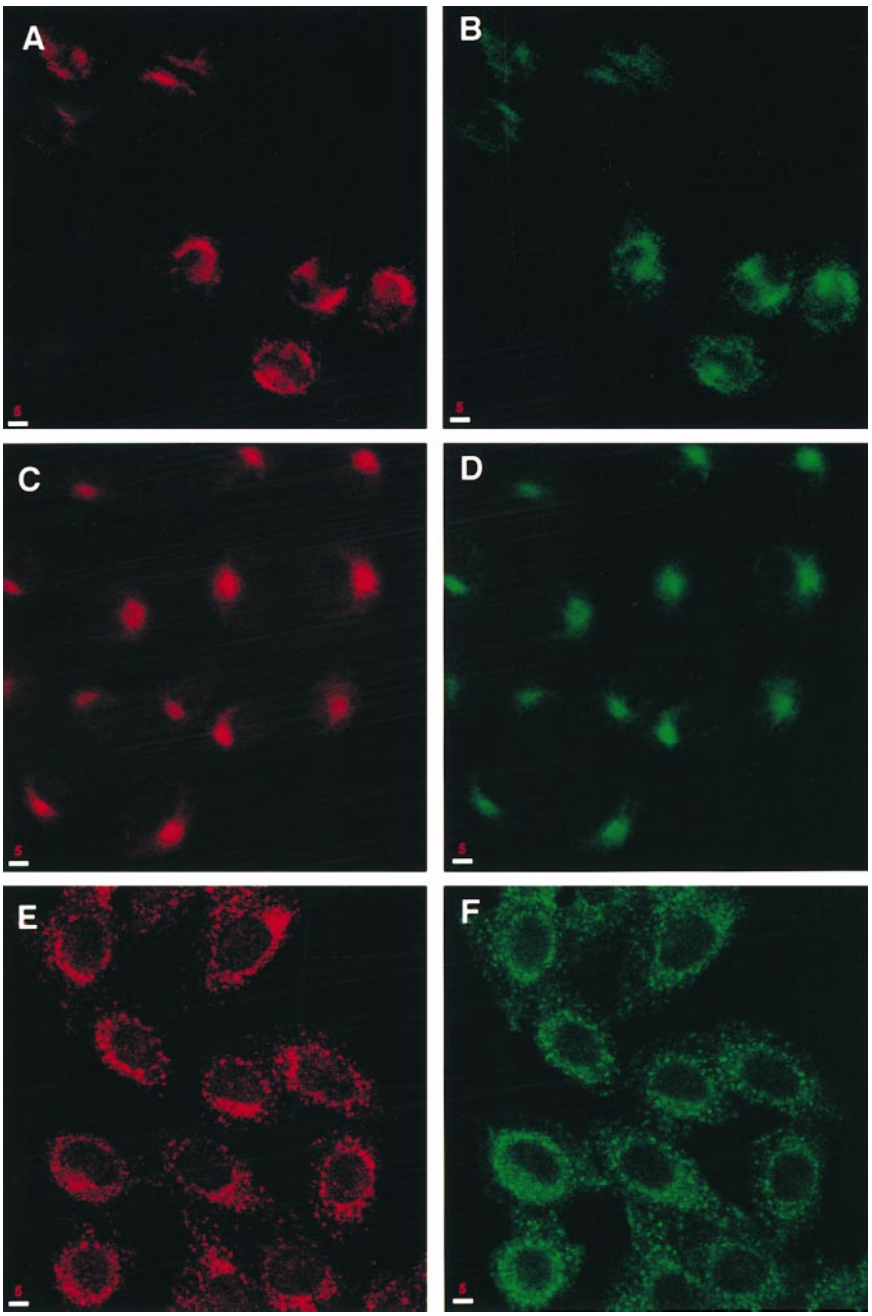

Figure 4. Brefeldin A and nocodazole alter the subcellular localization of syntaxin 13. NRK cells, untreated (*A* and *B*) or treated with 5 μg/ml BFA (*C* and *D*) or nocodazole (*E* and *F*), were fixed with 4% paraformaldehyde, permeabilized with saponin, and costained for syntaxin 13 (*A*, *C*, and *E*) and TfR (*B*, *D*, and *F*). This was followed by incubation with Texas red-labeled anti–rabbit IgG and FITC-labeled anti–mouse IgG antibodies before processing for confocal microscopy. Bars, 5 μm.

bling early and recycling endosomes, respectively (data not shown). PC12 cells were then extensively washed to remove nonspecifically bound Tf. After these washes only 5% of total Tf was associated to the plasma membrane, as determined by extraction of cells with 0.2 M glycine, pH 2.5. This labeling most likely represents Tf associated with plasma membrane TfR, since it could be reduced to almost undetectable levels (1.7% of total) by internalizing Tf for 15 min at 37°C. PC12 cells were then SLO permeabilized and incubated for 1 h on ice and then followed by four washes. These conditions were sufficient to wash out over 85% of cytosol as determined using a LDH detection system (Sigma Chemical Co.).

The recycling of [^{125}I]Tf was then initiated by incubating PC12 "ghosts" at 37°C in the presence or absence of cytosol as described in Materials and Methods. Recycled Tf is expressed as a percentage of total internalized Tf. Total Tf was calculated for every sample separately, and consisted of released, glycine-extractable (plasma membrane associated), and glycine-nonextractable (internalized) Tf. Plasma membrane-associated Tf in all cases was ~5% (data not shown). Recycling of [^{125}I]Tf was cytosol dependent, since the absence of cytosol resulted in about twofold reduction in Tf release (Fig. 7 *A*). The time course of Tf recycling closely resembled the recycling in intact PC12 cells (Fig. 8 *A*), as well as [^{125}I]IgG transcytosis and recycling reported in SLO-permeabilized MDCK cells expressing polymeric Ig receptor (2). The Tf recycling also required ATP and

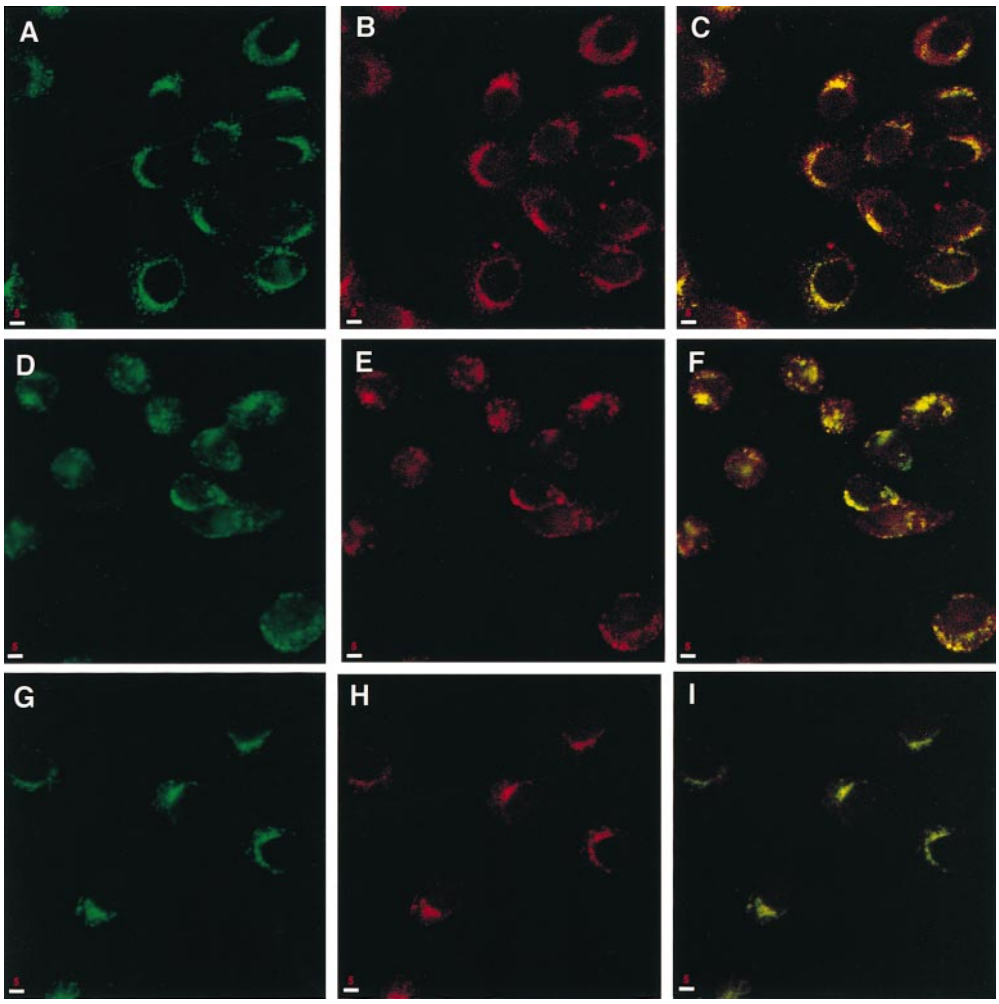

Figure 5. Syntaxin 13 localizes with internalized Tf at different temperatures. CHO cells were incubated with Texas Red-labeled Tf for 30 min at 37°C (*A–C*) or for 2.5 h at 15°C (*D–I*) and then either processed immediately (*A–F*) or washed and shifted to 37°C for 15 min (*G–I*). All cells were then fixed with 4% paraformaldehyde, immunostained for syntaxin 13, and then processed for confocal microscopy. (*A*, *D*, and *G*) Syntaxin 13; (*B*, *E*, and *H*) Tf-Texas red; (*C*, *F*, and *I*) merged images. *Yellow*, area of overlap. Bars, 5 μm.

was temperature dependent (Fig. 8 *B*). In the samples where ATP was substituted with nonhydrolyzable ATPγS, cytosol-dependent Tf recycling was reduced to background levels. Similarly, no cytosol-dependent release of [^{125}I]Tf was observed when samples containing cytosol and ATP were incubated at 4°C (Fig. 8 *B*). Moreover, NEM treatment also inhibited cytosol-dependent Tf release (Fig. 8 *B*). Thus, although we cannot formally exclude the possibility that NEM had its effect through proteins other then NSF, the data suggest that much of the Tf recycling as measured by this assay is mediated through SNARE-dependent fusion.

To determine whether syntaxin 13 is involved in TfR recycling, we tested the effect of polyclonal anti-syntaxin 13 antibody on the release of [^{125}I]Tf. PC12 "ghosts" were preincubated with 20 μg/ml antisyntaxin antibody as described in Materials and Methods, before initiating recycling by moving the samples to a 37°C water bath. As shown in Fig. 8 *B*, whole anti-syntaxin 13 antibody as well as anti-syntaxin 13 Fab fragments significantly reduced cytosol-dependent Tf recycling. The anti-syntaxin 13 antibody effect was concentration dependent with IC_{50} value at ~2 μg/ml (Fig. 8 *C*). Neither purified rabbit IgG nor anti-syntaxin 5 antibodies had any effect on the assay. Indeed, syntaxin 5 is a SNARE involved in ER to Golgi and intra-Golgi transport (24), thus it would not be expected to be involved in recycling of plasma membrane proteins. Interestingly, anti-syntaxin 1A antibody also had no effect on Tf recycling (Fig. 8 *B*), suggesting that the recycling of plasma membrane proteins and regulated secretion occur through two distinct pathways, which use different SNAREs. The anti-syntaxin 13 effect on Tf recycling was also tested using PC12 cells permeabilized by "cracking." As in SLO-permeabilized cells, anti-syntaxin 13 antibody inhibited Tf release, whereas IgG, anti-syntaxin 1A, and anti-syntaxin 5 had no effect (Fig. 8 *B*). To confirm the specificity of our assay, we tested the ability of syntaxin 13 to affect Ca^{2+}-dependent [^{3}H]norepinephrine exocytosis in "cracked" PC12 cells. Indeed, the anti-syntaxin 13 antibody had no effect on norepinephrine exocytosis (data not shown), suggesting that syntaxin 13 plays a role in plasma membrane recycling but not synaptic vesicle exocytosis.

Detergent-extracted Syntaxin 13 Forms a Stable and NSF/αSNAP-sensitive Protein Complex

A synaptic vesicle core complex consisting of syntaxin 1/VAMP 2/SNAP-25 interacts with NSF and αSNAP pro-

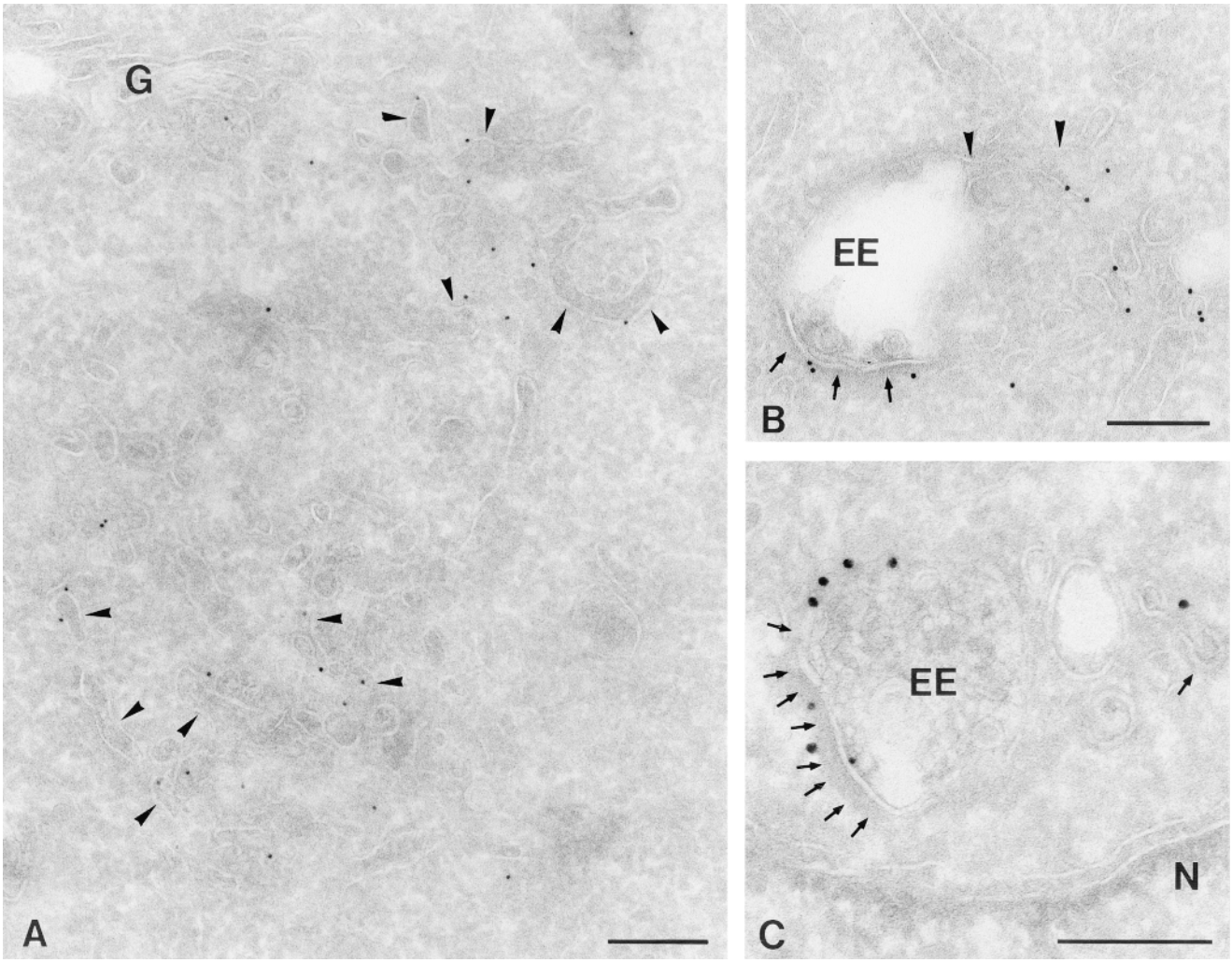

Figure 6. Ultrathin cryosections of CHO cells showing the subcellular localization of syntaxin 13. (*A* and *B*) Syntaxin 13 (10-nm gold) is present on extensive clusters of tubulovesicular membranes (*arrowheads* in *A*) located near Golgi (*G*) complex (*A*) or in association with early endosomes (*EE*). Sometimes continuities between EE vacuoles and syntaxin 13–positive tubules are seen (*arrowheads* in *B*). In addition, syntaxin 13 is found on EE vacuoles (*B*), often in parts of membrane that bear a dark cytosolic coating (*arrows*). (*C*) Double-immunogold labeling of syntaxin 13 (10-nm gold) and clathrin (15-nm gold) identifies the dark coating on the EE as clathrin. *N*, nucleus. Bars, 200 nm.

teins to form a larger complex which is dissociated by NSF ATPase upon ATP hydrolysis (55). NSF-dependent rearrangement of the fusion complex has also been demonstrated in several other vesicular trafficking pathways (24). To test whether syntaxin 13 is involved in the formation of a similar SNARE complex, we examined the distribution of syntaxin 13 using sedimentation velocity in continuous glycerol gradients in the presence or absence of αSNAP and NSF with ATP or ATPγS. As shown in Fig. 9 *A*, after fractionation of rat brain Triton X-100 extracts on 11–34% glycerol gradients, syntaxin 13 is present in fractions 2–9, with a peak near fraction 4 corresponding to ~67 kD. Although a significant pool of syntaxin 13 is clearly part of a protein complex, a substantial amount is apparently monomeric, since syntaxin 13 is also present in fractions 2 and 3. Similar results were also obtained by separating a brain detergent extract on 25–49% glycerol gradients (Fig. 9 *B*, *top*). When the extract was preincubated with recombinant NSF and αSNAP in the presence of ATPγS, a portion of syntaxin 13 shifted to fractions 8–10 (Fig. 9 *B*, *middle*), corresponding to ~660 kD. These data are consistent with the formation of a new complex which now includes NSF and αSNAP. When the extracts were preincubated with recombinant NSF and αSNAP under the conditions favoring ATP hydrolysis, syntaxin 13 shifted back to the slowly sedimenting fractions (Fig. 9 *B*, *bottom*). However, now syntaxin 13 was present in fractions 1–4, with the peak in fraction 2, corresponding to its expected sedimentation of its monomeric form (Fig. 9 *B*, *bottom*). Thus, as seen with other systems, NSF ATPase activity did not merely remove NSF and αSNAP from the complex, but also led to disassembly of the complex itself (Fig. 9 *B*, *bottom*).

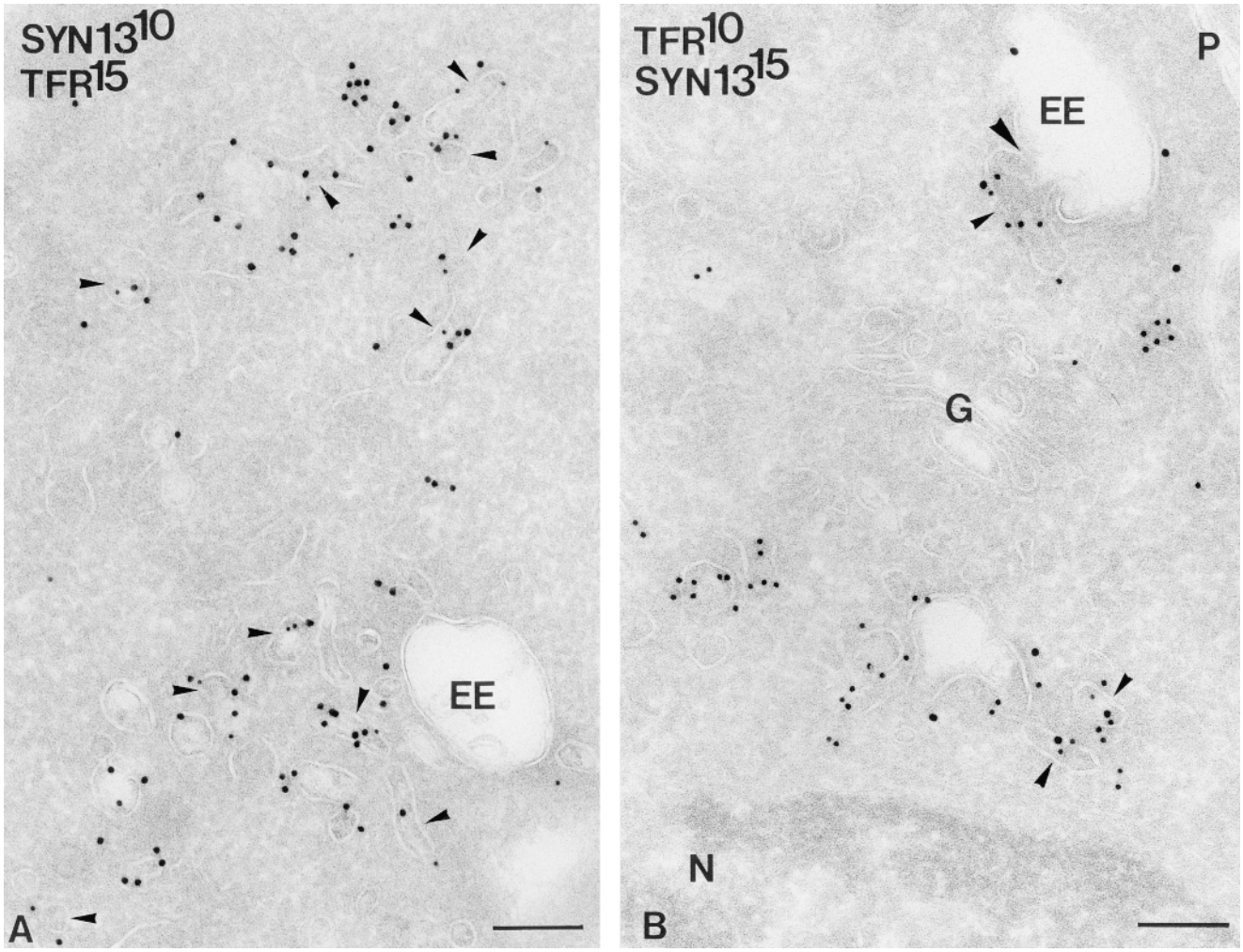

Figure 7. Double-immunogold labeling of syntaxin 13 and TfR (gold sizes are indicated on the pictures) showing extensive colocalization (*small arrowheads*) in the tubulovesicular membrane clusters. (*B*) *Large arrowhead*, a syntaxin 13/TfR-positive tubule connected with early endosome (*EE*) vacuole. *G*, Golgi complex; *N*, nucleus; *P*, plasma membrane. Bar, 200 nm.

Purification and Characterization of the Syntaxin 13 Trafficking Complex(es)

To further investigate the mechanism of syntaxin 13 function, we attempted to purify and identify components of the 67-kD complex. Immunoprecipitations from rat brain Triton X-100 extracts using affinity-purified anti-syntaxin 13 antibodies were scaled up to obtain sufficient quantities of protein to visualize by Coomassie staining of gels (Fig. 10). Each specific protein band was digested with trypsin and subjected to Edman sequence analysis (Table I).

As expected, the 38- and 30-kD protein bands yielded sequences corresponding to syntaxin 13 (Fig. 10 and Table I). Indeed the 38-kD protein band matched the size of full-length syntaxin 13, whereas the 30-kD protein band represents its degradation product as discussed earlier. The identity of both bands were also confirmed by immunoblotting (data not shown).

The peptide sequence from the 25-kD protein was identical to a region of SNAP-25 (Table I). Previous work identified SNAP-25 as a protein enriched in synaptic terminals and involved in exocytosis of synaptic vesicles (8, 42). Syntaxin 1 and VAMP2 were identified as major SNAP-25–binding partners (7, 55). Our finding that SNAP-25 is a member of a protein complex containing syntaxin 13 but lacking syntaxin 1, raises the possibly that this complex plays an important and unique role in synaptic transmission. Alternatively, SNAP-25 may also have a role other trafficking steps besides synaptic vesicle exocytosis.

The polypeptides from 20- and 18-kD bands were identical to regions of VAMP2 and VAMP3/cellubrevin proteins (Table I). Based on polypeptide sequences we could not differentiate between VAMP2 and VAMP3/cellubrevin, because of the high homology between these proteins. Moreover, the VAMP2 and VAMP3/cellubrevin domains known to be responsible for the interactions with syntaxins (31) are virtually identical suggesting that both VAMPs are capable of interacting with syntaxin 13. VAMP2 has been identified as a v-SNARE involved in synaptic vesicle exocytosis. Its association with syntaxin 13

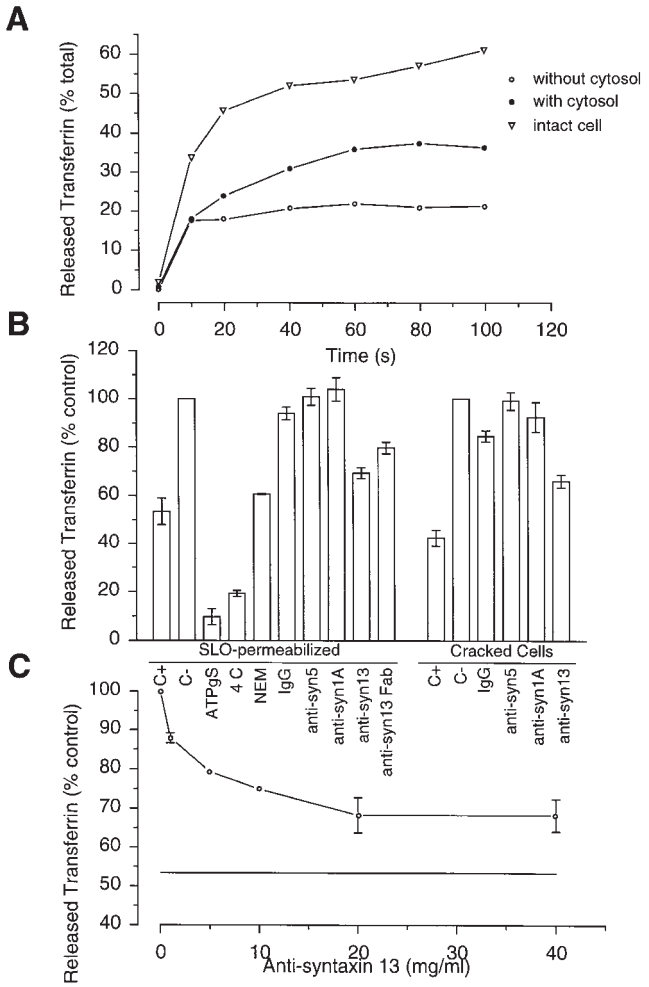

Figure 8. Syntaxin 13 functions in Tf recycling in permeabilized PC12 cells. Tf recycling was measured using SLO-permeabilized PC12 cells as described in Materials and Methods. To label early and recycling endosomes, PC12 cells were loaded with [^{125}I]Tf for 30 min at 37°C. (*A*) Intact (*open triangles*) or SLO-permeabilized PC12 cells were incubated with (*closed circles*) or without (*open circles*) cytosol for different periods of time. Total Tf was calculated as the sum of released, glycine-extractable, and glycine-nonextractable Tf. Data shown are the means of two independent experiments. (*B*) SLO-permeabilized or "cracked" PC12 cells were incubated without (*C−*) or with (remaining samples) cytosol for 2 h either at 4°C (*4°C*) or at 37°C (rest of the samples). Where indicated, cell "ghosts" were preincubated at 4°C for 1 h with either whole molecule (*anti-syn13*) or Fab fragments (*anti-syn13 Fab*) of anti-syntaxin 13, anti-syntaxin 5 (*anti-syn5*), anti-syntaxin 1A (*anti-syn1A*), or rabbit IgG (*IgG*). In addition, where indicated, cytosol was either incubated for 15 min on ice with 2 mM NEM (*NEM*) or ATP was replaced with ATPγS (*ATPγS*). The data shown are the means of three independent experiments ± SEM. (*C*) SLO-permeabilized PC12 cells were preincubated with varying concentrations of anti-syntaxin 13 antibody before measuring the release of Tf by incubation without or with cytosol for 2 h at 37°C. Data is expressed as the percentage of total cytosol dependent Tf release. The data shown are the means of three independent experiments ± SEM. *Straight line*, the levels of Tf release in the absence of cytosol.

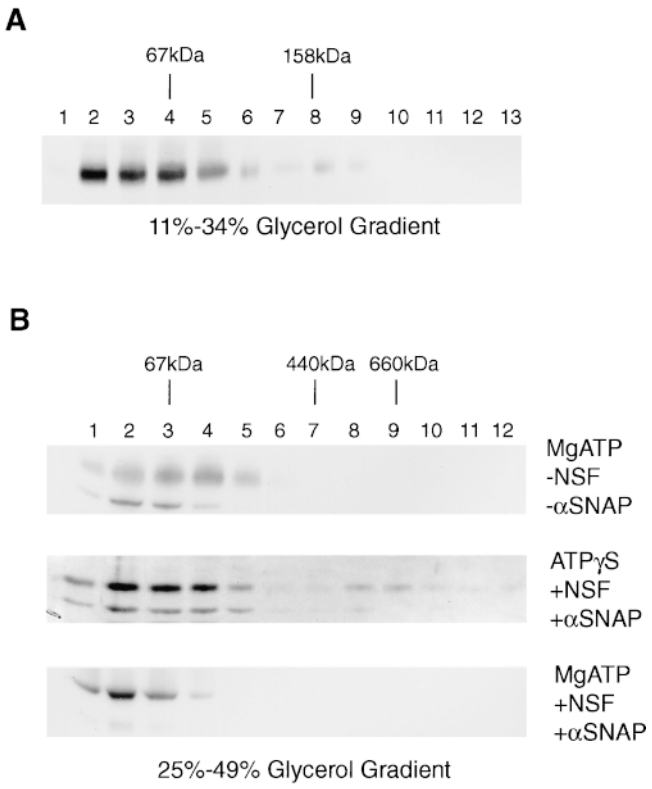

Figure 9. Syntaxin 13 forms a complex that is regulated by NSF/αSNAP. (*A*) Rat brain Triton X-100 extract was fractionated by velocity centrifugation through 11–34% glycerol gradient. Fractions were then separated by SDS-PAGE and analyzed by immunoblotting for the presence of syntaxin 13. (*B*) A rat brain Triton X-100 extract was incubated with (*middle* and *bottom*) or without (*top*) recombinant NSF and αSNAP under conditions blocking (*middle*) or allowing (*bottom*) NSF ATPase activity. Extracts were then fractionated through 25–49% glycerol velocity gradients and sequential fractions were analyzed by immunoblotting for the presence of syntaxin 13.

is consistent with the suggestion that syntaxin 13, SNAP-25, and VAMP2 form a complex in neurons important in synaptic vesicle recycling or exocytosis. VAMP3/cellubrevin, on the other hand, has been suggested to mediate endosomal trafficking and is enriched in RE (34), consistent with our data showing that syntaxin 13 plays a role in constitutive endosomal recycling.

The peptide sequences from the 33-kD band were identical to regions of βSNAP (Table I). α-, β-, and γ-SNAP proteins are necessary for NSF to associate with SNARE complexes as illustrated in Fig. 9. Whereas αSNAP is ubiquitously expressed in all tissues, βSNAP is restricted to neuronal tissues (65), consistent with our findings that the syntaxin 13 complex is dissociated by NSF action.

Discussion

We previously identified syntaxin 13 as a novel member of the syntaxin family and suggested its involvement in endosomal trafficking based on the post-Golgi localization of transfected myc-tagged protein (1). Moreover, syntaxin 13

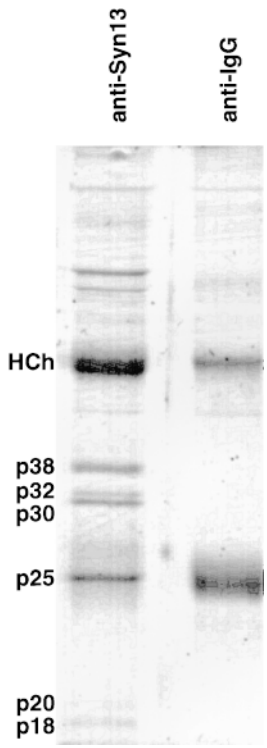

Figure 10. Rat brain syntaxin 13 forms a complex with βSNAP, SNAP-25, and VAMP2/3 proteins. Rat brain PNS was then extracted with 1% Triton X-100 and insoluble material was sedimented at 100,000 *g* for 1 h. For immunoprecipitations membrane extract was then preabsorbed for 2 h at 4°C with protein A–Sepharose beads. Immunoprecipitations were carried overnight at 4°C in the presence of affinity-purified anti-syntaxin 13 rabbit polyclonal antibody coupled to protein A–Sepharose. As a control, protein A–Sepharose coated with IgG was used. After the binding step the beads were washed four times with homogenization buffer containing 1% Triton X-100 (first three washes) or 0.2% Triton X-100 (final wash). Washed beads were then resuspended in SDS sample buffer and eluted proteins separated on SDS-PAGE. The indicated proteins were extracted from the gel and the amino acid sequence of peptides determined (Table I).

Table I. Peptide Sequences from Brain Syntaxin 13-associated Proteins

Protein band	Peptide sequences	Identity (residues)
kD		
38	ELGSLPLPLS	syntaxin 13 (76–85)
32	EEMFPAFTD	βSNAP (178–186)
	DYFFK	βSNAP (153–157)
	HDSATSFVDAGNAYK	βSNAP (28–42)
30	LQENLQQFQHSTNQLAK	syntaxin 13 (52–68)
25	KNLTDLGK	SNAP25 (76–83)
20	LSELDDRADALQAG	VAMP2/3 (47–60)
	ASQFETSA	VAMP2/3 (61–68)
18	LSELDDRADALQAGASQFET	VAMP2/3 (47–66)

The molecular weight of the protein band corresponds to that shown in Fig. 10. The peptide sequences obtained are listed along with the corresponding residue numbers in the identified proteins.

displays a high homology to syntaxin 7 (63, 66) and Pep12p (5), putative endosomal SNAREs in mammals and yeast. These observations were supported by the demonstration that endogenous syntaxin 13 is present on post-Golgi organelles leading to the suggestion that syntaxin 13 is localized to LE, where it might be involved in receiving vesicles from TGN and EE (57). In this study we present detailed localization and functional data demonstrating that endogenous syntaxin 13 resides on EE and REs, and functions in the recycling of internalized proteins to the plasma membrane.

Although the pathways of recycling through the endocytic pathway have been extensively characterized, the identity and function of the molecules that mediate this trafficking are just beginning to be understood. One of the main findings of the present study is that syntaxin 13 is highly concentrated in clusters of tubulovesicular membrane profiles, that also contain TfR. Membranes containing syntaxin 13 are partially interconnected and display clathrin-coated buds, suggesting a branched network of membranes morphologically identical to previously described EE tubules (18, 53, 58) and RE (28, 29). Whereas light-level fluorescence microscopy did not allow us to distinguish tubular EE from RE, electron microscopic ultrastructural studies revealed syntaxin 13 on peripheral as well as perinuclear tubular clusters suggesting that this SNARE is found in the tubulovesicular recycling network which includes tubular EE as well as RE. This hypothesis is supported by recent real-time videoimaging of NRK cells, which clearly demonstrates the presence of a highly dynamic network of vesicles and tubules that contain syntaxin 13 fused to the green fluorescent protein (data not shown). In addition, significant levels of syntaxin 13 are found on clathrin-coated regions of the EE vacuoles, suggesting that the protein uses the same EE exit sites as TfR. Furthermore, the vacuolar and tubular endosomal localization suggests that syntaxin 13 cycles between these compartments. Indeed, a currently favored model for protein recycling suggests that most proteins enter the common vacuolar EE and are then sorted to separate pathways leading to LE, tubular endosomes, or specialized exocytotic organelles, such as synaptic vesicles. At temperatures between 15° and 22°C, endocytosis still occurs whereas protein sorting at the EE level is significantly slowed (29, 59), resulting in accumulation of recycling proteins such as TfR, GLUT4, and synaptophysin in peripheral structures which most likely represent expanded vacuolar endosomes (51, 64). The accumulation of syntaxin 13 in the peripheral vacuolar organelles upon treatment with nocodazole or incubation at 15°C suggests a similar trafficking pathway for this SNARE protein. Another trafficking event within the endocytic cycle is the fusion of endosomes within the EE network, which may be homotypic fusion between vacuolar endosomes, or trafficking from vacoular EE to the tubulovesicular recycling network (11, 19). The localization of syntaxin 13 as well as its likely cycling between vacuolar EE and tubulovesicular recycling endosomes makes this SNARE a likely candidate to mediate endosome–endosome fusion.

To understand more fully the role of syntaxin 13 in endosomal recycling, we reconstituted TfR recycling in SLO-permeabilized PC12 cells and demonstrated that antibodies against syntaxin 13 significantly reduced the release of internalized Tf. We confirmed that the anti-syntaxin 13 effect on Tf recycling was not an artifact caused by SLO by repeating the assay using cell "cracking" as the means of permeabilization. Although the antibody inhibition was clearly significant, we never achieved complete inhibition of TfR cycling. The partial inhibition may indicate that some of the syntaxin 13 is in complexes that are not accessible to the antibodies. Alternatively, a portion of the TfR maybe shuttled to the plasma membrane directly from vacuolar EE, or a portion of the TfR may be transported along a parallel pathway mediated by SNAREs other than syntaxin 13. Although transit through vacuolar EE directly back to the plasma membrane is faster than trafficking

through tubulovesicular recycling endosomes (14, 49), the fraction of TfR that recycles directly from vacuolar EE remains unknown. Our data indicate that in PC12 cells at least half of the TfR recycles through tubular endosomes, since ~50% of Tf cycling in permeabilized cells is sensitive to anti-syntaxin 13 antibodies. This suggestion is further consistent with the observation that up to 75% of TfR is found in tubular endosomes (61). A final possibility for the partial block of Tf recycling is that the trafficking is not synchronized in our system and therefore some Tf may have already passed through tubular endosomes at the time we added the blocking antibody.

Taken together, the localization and functional data suggest that syntaxin 13 mediates protein recycling via tubulovesicular endosomes. Although further studies are needed to determine the precise site of syntaxin 13 function in protein recycling, we suggest that this SNARE most likely mediates the delivery of membranes to the tubulovesicular recycling network, consisting of tubular extensions of EE and RE. The source of these trafficking organelles is yet to be determined. One possibility is that syntaxin 13 mediates the trafficking of recycling proteins from the vacuolar early endosomes to the tubular endosomes, from where they are then recycled back to the plasma membrane. We have not ruled out the possibility that syntaxin 13 could also mediate the trafficking of unsorted proteins directly from the plasma membrane to the EE for the subsequent sorting and trafficking, either back to the plasma membrane, or to the lysosomal degradation pathway. Although it is clear that syntaxin 13 is necessary for the recycling of TfR, it is yet to be determined whether this SNARE functions in multiple trafficking steps. Indeed, a small but significant amount of syntaxin 13 is also present on the vacuolar endosomes, thus we cannot exclude the possibility that it might function in receiving the proteins destined to be degraded in the lysosomes.

Syntaxin 13 is likely to function through the formation of SNARE complexes which mediate late steps in the docking or fusion of membranes. We found syntaxin 13 in a complex with VAMP3/cellubrevin and/or VAMP2. VAMP3/cellubrevin appears to be concentrated on RE (14) where it is believed to function in TfR recycling (17) and it has become clear that VAMP2 is widely expressed in a variety of nonneuronal tissues, where it has an endosomal-like immunofluorescence staining pattern (48). Thus, it is likely that cellubrevin and/or VAMP2 function in protein recycling through associations with syntaxin 13.

Interestingly, syntaxin 13 also appears to form a complex with SNAP-25. SNAP-25 is largely present on the plasma membrane where it associates with syntaxin 1 to mediate plasma membrane vesicle fusion including exocytosis of neurotransmitter. Nevertheless, at least some of the syntaxin 13 seems to be associated with SNAP-25 since the proteins can be cross-linked in vivo (data not shown). SNAP-25 may be involved in TfR recycling in neuronal and neuroendocrine cells, however, anti–SNAP-25 antibodies failed to inhibit [I^{125}]Tf recycling in SLO-permeabilized PC12 cells. Thus, our data suggest an alternative possibility that the VAMP2–SNAP-25–syntaxin 13 complex may play a role in synaptic vesicle genesis and cycling. Indeed, neuronal staining demonstrates that syntaxin 13 is present in the axons where it colocalizes with synaptic vesicle markers (data not shown). Moreover, whereas a majority of SNAP-25 is localized on plasma membrane, ~20% is present on vesicles (56, 62) where it could interact with syntaxin 13. Further work, however, is required to determine the precise physiological role of the syntaxin 13 and SNAP-25 interaction. SNAP-23 is a SNAP-25 homologue in nonneuronal cells. It is likely that SNAP-23 interacts with syntaxin 13 in nonneural cells because SNAP-23 binds to syntaxin 13 in vitro (data not shown, also see ref. 57). Moreover, SNAP-23 has been implicated in basolateral recycling of TfR in SLO-permeabilized MDCK cells (32, 36). Although the majority of SNAP-23 is located on the plasma membrane where it interacts with syntaxin 4 and syntaxin 3, a small but significant amount is clearly also present on the endosome-like organelles, where it could interact with syntaxin 13 (32, 36). Our failure to coprecipitate SNAP-23 with syntaxin 13 from the PC-12 and rat brain Triton X-100 extracts, might be simply due to its relatively low amounts as compared with SNAP-25, and/or due to a transient nature of SNAP-23 interaction with syntaxin 13.

The contribution of SNARE pairing to the specificity of vesicle trafficking is still not clear. Clearly a set of SNAREs critical for ER to TGN trafficking are coimmunoprecipitated with antibodies against syntaxin 5 (24). However, antibodies against syntaxins 1, 6, and 13 all immunoprecipitate VAMP2/3 (9) and syntaxin 1 and syntaxin 13 antibodies coimmunoprecipitate SNAP-25. Based on this still limited data we hypothesize that there will be relatively few sets of SNAREs that form distinct core complexes. If this hypothesis is confirmed, little of the specificity of vesicle trafficking will be defined solely through SNARE pairing. This, of course, does not mean that SNARE proteins are not important in defining trafficking specificity. Whereas the highly conserved syntaxin H3 domain is sufficient for SNARE binding, the whole syntaxin molecule, and in particular amino-terminal domains, are necessary for the appropriate syntaxin localization (41). Perhaps interactions of SNAREs with other proteins such as Rabs and their effectors will be critical in defining the fidelity of fusion events, and the formation of SNARE complexes will be downstream of these specificity events. It will be interesting to see whether proteins known to be modulators of membrane trafficking through EE (rab5, rabaptin, EEA1), or RE (rab11) can directly or indirectly associate with syntaxin 13, and in this way regulate its localization and binding properties (11, 19, 52).

Although considerable advances have been made in studying vesicular trafficking, our understanding of the organization of the endocytic pathway is still fragmentary. This is evident from the very diverse and often conflicting interpretations originating from different experimental approaches to studying the same endocytic trafficking steps. Thus, the identification of syntaxin 13 as a SNARE mediating the recycling protein flow through tubulovesicular recycling endosomes is likely to pave the way for further understanding of the processes regulating the endosomal sorting and recycling of the proteins.

We would like to acknowledge D. Foletti (Stanford University, Stanford, CA) for his help in culturing embryonic hippocampal neurons. We also thank M. Steegmaier (Stanford University) for assistance in hybridoma culturing and R. Winant of the Stanford PAN facility for amino acid se-

quencing. We thank W. Stoorvogel (University of Utrecht, Utrecht, The Netherlands) for providing useful suggestions on the recycling assay and the critical reading of the manuscript. We would also like to thank C. Hazuka for the critical reading of the manuscript. M. Niekerk, R. Scriwanek, and T. van Rijn (all from University of Utrecht) are acknowledged for the preparation of the electronmicrographs. V. Oorschot (University of Utrecht) is gratefully acknowledged for the preparation of ultrathin cryosections.

Received for publication 5 August 1998 and in revised form 7 October 1998.

References

1. Advani, R.J., H.R. Bae, J.B. Bock, D.S. Chao, Y.C. Doung, R. Prekeris, J.S. Yoo, and R.H. Scheller. 1998. Seven novel mammalian SNARE proteins localize to distinct membrane compartments. *J. Biol. Chem.* 273: 10317–10324.
2. Apodaca, G., M.H. Cardone, S.W. Whiteheart, B.R. dasGupta, and K.E. Mostov. 1996. Reconstitution of transcytosis in SLO-permeabilized MDCK cells: existence of an NSF-dependent fusion mechanism with the apical surface of MDCK cells. *EMBO (Eur. Mol. Biol. Organ.) J.* 15: 1471–1481.
3. Banker, G.A., and M.W. Cowan. 1977. Rat hippocampal neurons in dispersed cell culture. *Brain Res*. 126:397–425.
4. Bean, A.J., R. Seifer, Y.A. Chen, R. Sacks, and R.H. Scheller. 1998. Hrs-2 is an ATPase implicated in calcium-regulated secretion. *Nature*. 385:826–829.
5. Becherer, K.A., S.E. Rieder, S.D. Emr, and E.W. Jones. 1996. Novel syntaxin homologue, Pep12p, required for the sorting of lumenal hydrolases to the lysosome-like vacuole in yeast. *Mol. Biol. Cell*. 7:579–594.
6. Bennett, M.K., and R.H. Scheller. 1993. The molecular machinery for secretion is conserved from yeast to neurons. *Proc. Natl. Acad. Sci. USA*. 90:2559–2563.
7. Bennett, M.K., and R.H. Scheller. 1994. A molecular description of synaptic vesicle membrane trafficking. *Annu. Rev. Biochem*. 63:63–100.
8. Binz, T., J. Blasi, S. Yamasaki, A. Baumeister, E. Link, T.C. Sudhof, R. Jahn, and H. Niemann. 1994. Proteolysis of SNAP-25 by types E and A botulinal neurotoxins. *J. Biol. Chem*. 269:1617–1620.
9. Bock, J.B., J. Klumperman, S. Davanger, and R.H. Scheller. 1997. Syntaxin 6 functions in trans-Golgi network vesicle trafficking. *Mol. Biol. Cell*. 8:1261–1271.
10. Bock, J.B., R.C. Lin, and R.H. Scheller. 1996. A new syntaxin family member implicated in targeting of intracellular transport vesicles. *J. Biol. Chem*. 271:17961–17965.
11. Bucci, C., R.G. Parton, I.H. Mather, H. Stunnenberg, K. Simons, B. Hoflack, and M. Zerial. 1992. The small GTPase rab5 functions as a regulatory factor in the early endocytic pathway. *Cell*. 70:715–728.
12. Chang, M.P., W.G. Mallet, K.E. Mostov, and F.M. Brodsky. 1993. Adaptor self-aggregation, adaptor-receptor recognition and binding of alpha-adaptin subunits to the plasma membrane contribute to recruitment of adaptor (AP2) components of clathrin-coated pits. *EMBO (Eur. Mol. Biol. Organ.) J.* 12:169–180.
13. Deleted in proof.
14. Daro, E., P. van der Sliujis, T. Galli, and I. Mellman. 1996. Rab4 and cellubrevin define distinct populations of endosomes on the pathway of transferrin recycling. *Proc. Natl. Acad. Sci. USA*. 93:9559–9564.
15. Darsow, T., S.E. Rieder, and S.D. Emr. 1997. A multispecifisity syntaxin homologue, Vam3p, essential for autophagic and biosynthetic proteinm transport to the vacuole. *J. Cell Biol.* 138:517–529.
16. Dunn, K.W., S. Mayor, and J.N. Myers. 1994. Application of ration fluorescence microscopy in the study of cell physiology. *FASEB (Fed. Am. Soc. Exp. Biol.) J.* 8:573–582.
17. Galli, T., T. Chilcote, O. Mundigl, T. Binz, H. Niemann, and P. de Camilli. 1994. Tetanus toxin-mediated cleavage of cellubrevin impairs exocytosis of transferrin receptor-containing vesicles in CHO cells. *J. Cell Biol*. 125: 1015–1024.
18. Geuze, H.J., J.W. Slot, G.J. Strous, J. Peppard, K. von Figura, A. Hasilik, and A.L. Schwartz. 1984. Intracellular receptor sorting during endocytosis: comparative immunoelectron microscopy of multiple receptors in rat liver. *Cell*. 37:195–204.
19. Gorvel, J.P., P. Chavrier, M. Zerial, and J. Gruenberg. 1991. rab5 controls early endosome fusion in vitro. *Cell*. 64:915–925.
20. Gosh, R.N., D.L. Gelman, and F.R. Maxfield. 1994. Quantification of low density lipoproteins and transferrin endocytic sorting in HEp2 cells using confocal microscopy. *J. Cell Sci.* 107:2177–2189.
21. Gruenberg, J., and F.R. Maxfield. 1995. Membrane transport in the endocytic pathway. *Curr. Opin. Cell Biol.* 7:552–563.
22. Hanson, P.I., R. Roth, H. Morisaki, R. Jahn, and J.E. Heuser. 1997. Structure and conformational changes in NSF and its membrane receptor complexes visualized by quick-freeze/deep-etch electron microscopy. *Cell*. 90:523–535.
23. Hay, J., and T.F.J. Martin. 1992. Resolution of regulated secretion into sequential MgATP-dependent and Calcium-dependent stages mediated by distinct cytosolic factors. *J. Cell Biol.* 119:139–151.
24. Hay, J.C., D.S. Chao, C.S. Kuo, and R.H. Scheller. 1997. Protein interactions regulating vesicle transport between the endoplasmic reticulum and Golgi apparatus in mammalian cells. *Cell*. 89:149–158.
25. Hay, J.C., H. Hirling, and R.H. Scheller. 1996. Mammalian vesicle trafficking proteins of the endoplasmic reticulum and Golgi apparatus. *J. Biol. Chem*. 271:5671–5679.
26. Helenius, A., I. Mellman, D. Wall, and A. Hubbart. 1983. Endosomes. *Trends Biochem. Sci.* 8:245–250.
27. Hopkins, C.R. 1983. Intracellular routing of transferrin receptors in epidermoid carcinoma A431 cells. *Cell*. 35:321–330.
28. Hopkins, C.R., A. Gibson, M. Shipman, and K. Miller. 1990. Movement of internalized ligand-receptor complexes along a continuous endosomal reticulum. *Nature*. 346:335–339.
29. Hopkins, C.R., and I.S. Trowbridge. 1983. Internalization and processing of transferrin and transferrin receptor in human carcinoma A431 cells. *J. Cell Biol.* 97:508–521.
30. Inoue, A., and K. Akagawa. 1993. Neuron specific expression of a membrane protein, HPC-1: tissue distribution, and cellular and subcellular localization of immunoreactivity and mRNA. *Brain Res. Mol. Brain. Res*. 19:121–128.
31. Kee, Y., R.C. Lin, S.C. Hsu, and R.H. Scheller. 1995. Distinct domains of syntaxin are required for synaptic vesicle fusion complex formation and dissociation. *Neuron*. 14:991–998.
32. Leung, S.M., D. Chen, B.R. dasGupta, S.W. Whiteheart, and G. Apodaca. 1998. SNAP-23 requirement for transferrin recycling in streptolysin-O-permeabilized Madin-Darby canine kidney cells. *J. Biol. Chem*. 273: 17732–17741.
33. Lin, R.C., and R.H. Scheller. 1997. Structural organization of the synaptic exocytosis core complex. *Neuron*. 19:1087–1094.
34. Link, E., H. McMahon, G. Fisher von Mollard, S. Yamasaki, H. Niemann, T.C. Sudhof, and R. Jahn. 1993. Cleavage of cellubrevin by tetanus toxin does not affect fusion of early endosomes. *J. Biol. Chem.* 268:18423–18426.
35. Lippincott-Schwartz, J., L.C. Yuan, C. Tipper, M. Amherdt, L. Orci, and R. Klausner. 1991. Brefeldin A's effects on endosomes, lysosomes, and the TGN suggest a general mechanism for regulating organelle structure and membrane traffic. *Cell*. 67:601–616.
36. Low, S.H., S.J. Chapin, C. Wimmer, S.W. Whiteheart, L.G. Komuves, K.E. Mostov, and T. Weimbs. 1998. The SNARE machinery is involved in apical plasma membrane trafficking in MDCK cells. *J. Cell Biol*. 141:1503–1513.
37. Mayor, S., J.F. Presley, and F.R. Maxfield. 1993. Sorting of membrane components from endosomes and subsequent recycling to the cell surface. *J. Cell Biol.* 121:1257–1269.
38. Mellman, I. 1996. Endocytosis and molecular sorting. *Annu. Rev. Cell Dev. Biol.* 12:575–625.
39. Miettinen, J.M., K. Matter, W. Hunziker, J.K. Rose, and I. Mellman. 1992. Fc receptors contain a cytoplasmic domain determinant that actively regulates coated pit localization. *J. Cell Biol.* 118:875–888.
40. Nichols, B.J., C. Ungermann, H.R. Pelham, W.T. Wickner, and A. Haas. 1997. Homotypic vacuolar fusion mediated by t- and v-SNAREs. *Nature*. 387:199–202.
41. Nicholson, K.L., M. Munson, R.B. Miller, T.J. Filip, R. Fairman, and F.M. Hughson. 1998. Regulation of SNARE complex assembly by an N-terminal domain of the t-SNARE Sso1p. *Nat. Struct. Biol*. 5:793–802.
42. Oyler, G.A., G.A. Higgins, R.A. Hart, E. Battenberg, M. Billingsley, F.E. Bloom, and M.C. Wilson. 1989. The identification of a novel synaptosomal-associated protein, SNAP-25, differentially expressed by neuronal subpopulations. *J. Cell Biol*. 109:3039–3052.
43. Pearse, B.M. 1987. Clathrin and coated vesicles. *EMBO (Eur. Mol. Biol. Organ.) J.* 6:2507–2512.
44. Pearse, B.M., and M.S. Robinson. 1990. Clathrin, adaptors, and sorting. *Annu. Rev. Cell Biol*. 6:151–171.
45. Reaves, B., and G. Banting. 1992. Perturbation of the morphology of the *trans*-Golgi network following brefeldin A treatment: redistribution of a TGN-specific integral membrane protein TGN38. *J. Cell Biol.* 116:85–94.
46. Robinson, M.S., and T.E. Kreis. 1992. Recruitment of coat proteins onto Golgi membranes in intact and permeabilized cells: effect of brefeldin A and G protein activators. *Cell*. 69:129–138.
47. Robinson, M.S., C. Watts, and C. Zerial. 1996. Membrane dynamics in endocytosis. *Cell*. 84:13–21.
48. Rossetto, O., L. Gorza, G. Schiavo, N. Schiavo, R.H. Scheller, and C. Montecucco. 1996. VAMP/synaptobrevin usoforms 1 and 2 are widely and differentially expressed in nonneuronal tissues. *J. Cell Biol*. 132:167–179.
49. Schmid, S.L. 1988. Two distinct subpopulations of endosomes involved in membrane recycling and transport to lysosomes. *Cell*. 52:73–83.
50. Schmid, S.L., and E. Smythe. 1991. Stage-specific assays for coated pit formation and coated vesicle budding in vitro. *J. Cell Biol.* 114:869–880.
51. Schmidt, A., M.J. Hannah, and W.B. Huttner. 1997. Synaptic-like microvesicles of neuroendocrine cells originate from novel compartment that is continuous with plasma membrane and devoid of transferrin receptor. *J. Cell Biol*. 137:445–458.
52. Simonsen, A., R. Lippe, S. Christoforidis, J.M. Gaullier, A. Brech, J. Cal-

laghan, B.H. Toh, C. Murphy, M. Zerial, and H. Stenmark. 1998. EEA1 links PI(3)K function to rab5 regulation of endosome fusion. *Nature*. 394: 494–498.
53. Slot, J.W., H.J. Geuze, S. Gigengack, G.E. Lienhard, and D.E. James. 1991. Immunolocalization of the insulin regulatable glucose transporter in brown adipose tissue of the rat. *J. Cell Biol*. 113:123–135.
54. Sollner, T., M.K. Bennett, S.W. Whiteheart, R.H. Scheller, and J.E. Rothman. 1993. A protein assembly-disassembly pathway in vitro that may correspond to sequential steps of synaptic vesicle docking, activation, and fusion. *Cell*. 75:409–418.
55. Sollner, T., S.W. Whiteheart, M. Brunner, H. Erdjument-Bromage, S. Geromanos, P. Tempst, and J.E. Rothman. 1993. SNAP receptors implicated in vesicle targeting and fusion [see *Comments*]. *Nature*. 362:318–324.
56. Tagaya, M., S. Toyonaga, M. Takahashi, A. Yamamoto, T. Fujiwara, K. Akagawa, Y. Moriyama, and S. Mizushima. 1995. Syntaxin 1 (HPC-1) is associated with chromaffin granules. *J. Biol Chem*. 270:15930–15933.
57. Tang, B.L., A.E.H. Tan, L.K. Lim, S.S. Lee, D.Y.H. Low, and W. Hong. 1998. Syntaxin 12, a member of syntaxin family localized to the endosome. *J. Biol. Chem.* 273:6944–6950.
58. Tooze, J., and H. Hollinshead. 1991. Tubular early endosomal networks in AtT20 and other cells. *J. Cell Biol*. 115:635–653.
59. Trowbridge, I.S., J.F. Collawn, and C.R. Hopkins. 1993. Signal-dependent membrane protein trafficking in the endocytic pathway. *Annu. Rev. Cell. Biol.* 9:129–161.
60. Ulrich, O., S. Reinsch, S. Urbe, M. Zerial, and R.G. Parton. 1996. Rab11 regulates recycling through the pericentriolar recycling endosome. *J. Cell Biol.* 135:913–924.
61. van der Sluijs, P., M. Hull, P. Webster, P. Male, B. Goud, and I. Mellman. 1992. The small GTP-binding protein rab4 controls an early sorting event on the endocytic pathway. *Cell*. 70:729–740.
62. Walch-Solimena, C., J. Blasi, L. Edelmann, E.R. Chapman, G.F. von Mollard, and R. Jahn. 1995. The t-SNAREs syntaxin 1 and SNAP-25 are present on organelles that participate in synaptic vesicle recycling. *J. Cell Biol*. 128:637–645.
63. Wang, H., L. Frelin, and J. Pevsner. 1997. Human syntaxin 7: a Pep12p/Vps6p homologue implicated in vesicle trafficking to lysosomes. *Gene*. 199:39–48.
64. Wei, M.L., F. Bonzelius, R.M. Scully, R.B. Kelly, and G.A. Herman. 1998. GLUT4 and transferrin receptor are differentially sorted along the endocytic pathway in CHO cells. *J. Cell Biol.* 140:565–575.
65. Whiteheart, S.W., I.C. Griff, M. Brunner, D.O. Clary, T. Mayer, S.A. Buhrow, and J.E. Rothman. 1993. SNAP family of NSF attachment proteins includes a brain-specific isoform [see *Comments*]. *Nature*. 362:353–355.
66. Wong, S.H., Y. Xu, T. Zhang, and W. Hong. 1998. Syntaxin 7, a novel syntaxin member associated with the early endosomal compartment. *J. Biol. Chem.* 273:375–380.
67. Yamashiro, D., B. Tycko, S. Fluss, and F.R. Maxfield. 1984. Segregation of transferrin to a mildly acidic (pH 6.5) para-Golgi compartment in the recycling pathway. *Cell*. 37:789–800.